

Macalester College

From the Selected Works of John Cannon

June 20, 2004

Extended tidal structure in two Ly α -emitting starburst galaxies

John M Cannon, *University of Minnesota*

E D Skillman, *University of Minnesota*

D Kunth

C Leitherer

M Mas-Hesse, et al.



Available at: https://works.bepress.com/john_cannon/10/

EXTENDED TIDAL STRUCTURE IN TWO $\text{Ly}\alpha$ -EMITTING STARBURST GALAXIES

JOHN M. CANNON AND EVAN D. SKILLMAN

Department of Astronomy, University of Minnesota, 116 Church Street SE, Minneapolis, MN 55455; cannon@astro.umn.edu, skillman@astro.umn.edu

DANIEL KUNTH

Institut d'Astrophysique de Paris, 98bis Boulevard Arago, F-75014, Paris, France; kunth@iap.fr

CLAUS LEITHERER

Space Telescope Science Institute, 3700 San Martin Drive, Baltimore, MD 21218; leitherer@stsci.edu

MIGUEL MAS-HESSE

Centro de Astrobiología (CSIC-INTA), E-28850 Torrejon de Ardoz, Madrid, Spain; mm@laeff.esa.es

GÖRAN ÖSTLIN

Stockholm Observatory, SE-106 91 Stockholm, Sweden; ostlin@astro.su.se

AND

ARTASHES PETROSIAN

Byurakan Astrophysical Observatory and Isaac Newton Institute of Chile, Armenian Branch, Byurakan 378433, Armenia; artptrs@yahoo.com

Received 2003 December 16; accepted 2004 March 5

ABSTRACT

We present new Very Large Array (VLA) C-configuration H I imaging of the $\text{Ly}\alpha$ -emitting starburst galaxies Tol 1924–416 and IRAS 08339+6517. The effective resolution probes neutral gas structures larger than 4.7 kpc in Tol 1924–416 and larger than 8.1 kpc in IRAS 08339+6517. Both systems are revealed to be tidally interacting: Tol 1924–416 with ESO 338–IG04B ($6.6 = 72$ kpc minimum separation), and IRAS 08339+6517 with 2MASX J08380769+6508579 ($2.4 = 56$ kpc minimum separation). The H I emission is extended in these systems, with tidal tails and debris between the target galaxies and their companions. Since $\text{Ly}\alpha$ emission has been detected from both of these primary systems, these observations suggest that the geometry of the interstellar medium is one of the factors affecting the escape fraction of $\text{Ly}\alpha$ emission from starburst environments. Furthermore, these observations argue for the importance of interactions in triggering massive star formation events.

Subject headings: galaxies: individual (Tol 1924–416, IRAS 08339+6517) — galaxies: interactions — galaxies: starburst

1. INTRODUCTION

Here, we present new Very Large Array (VLA) H I imaging of the starburst galaxies Tol 1924–416 [α, δ (J2000.0) = $19^{\text{h}}27^{\text{m}}58^{\text{s}}.2, -41^{\circ}34'32''$; $D = 37.5$ Mpc; Östlin et al. 1998] and IRAS 08339+6517 [α, δ (J2000.0) = $08^{\text{h}}38^{\text{m}}23^{\text{s}}.2, 65^{\circ}07'15''$; $D \simeq 80$ Mpc, assuming $H_0 = 72$ km s $^{-1}$ Mpc $^{-1}$; Freedman et al. 2001]. Both galaxies reveal extended tidal structure in neutral hydrogen and are clearly interacting with nearby companions. Each appears to provide evidence for tidally induced starburst episodes.

These two systems were chosen for imaging because they exhibit prominent $\text{Ly}\alpha$ emission (Leitherer et al. 1995, 2002; Giavalisco et al. 1996; Kunth et al. 1998). Hydrogen $\text{Ly}\alpha$ is one of the most important diagnostic emission lines in astrophysics. It is predicted to be luminous in star-forming galaxies (Charlot & Fall 1993) and could potentially be used as an indicator of star formation activity in high-redshift systems. However, this application is not straightforward, since the propagation of $\text{Ly}\alpha$ photons in starburst galaxies appears to be a complex process that depends on many factors intrinsic to both the starburst itself (e.g., star formation rate, metallicity) and to the surrounding galaxy (e.g., geometry, kinematics, and dust content).

In a large spectroscopic sample of comparatively high-redshift Lyman break galaxies (LBGs; these systems have typical star formation rates $\geq 10 M_{\odot} \text{ yr}^{-1}$ and are thus directly comparable to more local “starburst” galaxies), Shapley et al.

(2003) find various correlations between the emergent $\text{Ly}\alpha$ profile (i.e., strengths of absorption or emission) and characteristics of the interstellar medium (ISM). In particular, dustier galaxies have less prominent $\text{Ly}\alpha$ emission, or equivalently, redder UV continuum slopes. $\text{Ly}\alpha$ emission strength is shown to anticorrelate with the kinematic offset implied by the redshift difference between $\text{Ly}\alpha$ emission and low-ionization interstellar absorption lines; that is, systems with larger outflow speeds usually show less prominent $\text{Ly}\alpha$ emission. Finally, systems with stronger $\text{Ly}\alpha$ emission show lower star formation rates on average than systems with weaker $\text{Ly}\alpha$ emission. These correlations suggest that many factors can contribute to the escape fraction of $\text{Ly}\alpha$ from starburst regions.

One of the most important factors that influences $\text{Ly}\alpha$ propagation is resonant scattering. It is well known that because of high resonant scattering by neutral hydrogen in the ISM, $\text{Ly}\alpha$ photons can be attenuated even by small amounts of dust. It is then expected that only young, relatively dust-free galaxies should be prodigious sites of $\text{Ly}\alpha$ production. Low-metallicity starburst galaxies in the local universe can be considered nearby analogs to such objects, which are expected in greater numbers at higher redshifts. Thus, it was surprising that *Hubble Space Telescope* (HST) observations of the most metal-poor galaxy known, I Zw 18, showed only damped $\text{Ly}\alpha$ absorption and no emission (Kunth et al. 1994). In stark contrast, the more metal-rich starburst galaxy Haro 2 showed prominent $\text{Ly}\alpha$ emission (Lequeux et al. 1995).

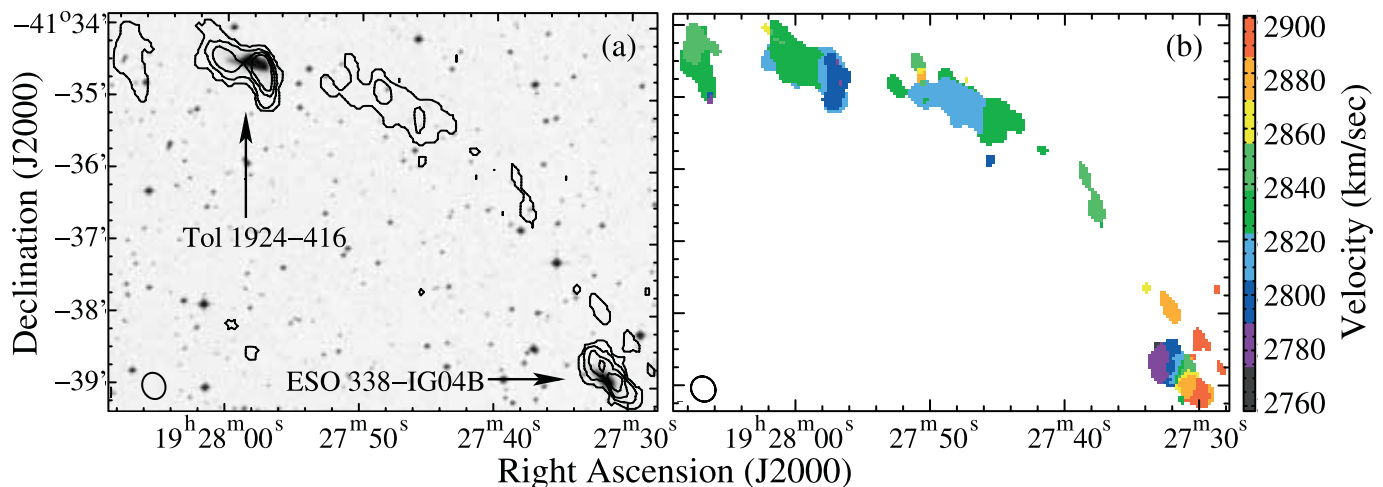


FIG. 1.—(a) DSS image of Tol 1924–416 overlaid with contours of the H I zeroth-moment image. Contours correspond to column densities of $(7.3, 29, 51, 73) \times 10^{20} \text{ cm}^{-2}$. Each galaxy is labeled; beam size is shown in the lower left corner. (b) Intensity-weighted velocity field of Tol 1924–416; it is apparent that H I is being removed from one or both systems. A component of solid-body rotation also remains within the optical extent of both galaxies. Beam size is shown in the lower left corner.

The effects of resonant scattering may be lessened if there is a velocity difference between the site of Ly α emission and the surrounding material from which resonant scattering can occur. This will Doppler shift the Ly α photon out of resonance and increase its chance of escaping the surrounding ISM. While this process seems to be complicated (note, e.g., that higher outflow speeds suggest less prominent Ly α emission profiles in the sample of Shapley et al. 2003), it appears that an important factor is the presence or absence of an outflow (see below). Indeed, Shapley et al. (2003) measure an average Ly α offset of greater than 300 km s^{-1} for the sample of Ly α -emitting LBGs. These observations and the studies of Giavalisco et al. (1996) and Kunth et al. (1998) argue for the importance of ISM geometry and kinematics in affecting the Ly α escape fraction.

The studies of Kunth et al. (1998), Tenorio-Tagle et al. (1999), and Mas-Hesse et al. (2003) have examined the characteristics of the ISM kinematics that appear to influence the propagation of Ly α photons in star-forming galaxies. If static, homogeneous neutral gas with column densities $\gtrsim 10^{18} \text{ cm}^{-2}$ shields the ionized gas, no emission will be detected. The resonant scattering of the Ly α photons will lead to increased probability of destruction by any dust that is present. On the other hand, there may be diffuse Ly α emission that is detectable on sight lines not coincident with the sources of UV photons. Similarly, if the areal coverage of the neutral gas is not uniform but clumpy, some Ly α emission may be detectable on favorable sightlines. Finally, if the velocity structure of the neutral gas is not static but rather outflowing from the ionizing regions (outflow velocities $\gtrsim 200 \text{ km s}^{-1}$), Ly α photons to the red of 1216 \AA can escape and Ly α emission may be significant. This explains the strong Ly α emission detected in some starburst galaxies with complete spatial coverage by neutral gas that is also comparatively rich in both metals and dust.

These observations were undertaken with these arguments in mind. Our group has obtained new *HST* Advanced Camera for Surveys (ACS) imaging of the Ly α line in a small sample of galaxies (see Kunth et al. 2003), two of which are Tol 1924–416 and IRAS 08339+6517. While these data are only a small segment of the sample that was imaged in Ly α ,

they will aid in the interpretation of the Ly α data. We note that our H I imaging sample does not include systems showing only Ly α absorption, so we must await a larger sample to draw definitive conclusions on the correlation between H I kinematics and the appearance of Ly α emission. However, the results presented here support the scenario that the geometry and kinematics of the ISM are important (although not the only) factors that affect the escape probability of Ly α photons from massive star formation regions.

2. OBSERVATIONS AND DATA REDUCTION

The NRAO VLA¹ was used to obtain H I spectral line data for these two systems, as part of observing program AC 654. Tol 1924–416 was observed in the BnC configuration for 180 minutes on 2002 September 30, while IRAS 08339+6517 was observed in the C configuration for 370 minutes on 2002 December 8 and 9. The correlator configuration yields a bandwidth of 3.125 MHz, with 64 channels separated by 48.8 kHz (10.5 km s^{-1}). The data were reduced and calibrated using standard methods in the AIPS environment. The data were imaged using uniform weighting; the single-plane rms noise is $1.3 \text{ mJy Beam}^{-1}$ for Tol 1924–416 and $0.40 \text{ mJy Beam}^{-1}$ for IRAS 08339+6517. With the final beam sizes ($26'' \times 16''$ for Tol 1924–416 and $21'' \times 16''$ for IRAS 08339+6517), this noise level implies single-plane 3σ detection thresholds of $2.3 \times 10^{20} \text{ cm}^{-2}$ and $6.9 \times 10^{19} \text{ cm}^{-2}$ for Tol 1924–416 and IRAS 08339+6517, respectively.

3. H I DATA: EXTENDED TIDAL STRUCTURE

With these data we detect extended tidal structure in each of these systems. In both cases H I gas is detected in the target system, in a neighboring galaxy, and in tidal material.

3.1. Tol 1924–416

In Figure 1 we present contours of the zeroth-moment (total column density) image overlaid on a Digitized Sky Survey

¹ The National Radio Astronomy Observatory is a facility of the National Science Foundation operated under cooperative agreement by Associated Universities, Inc.

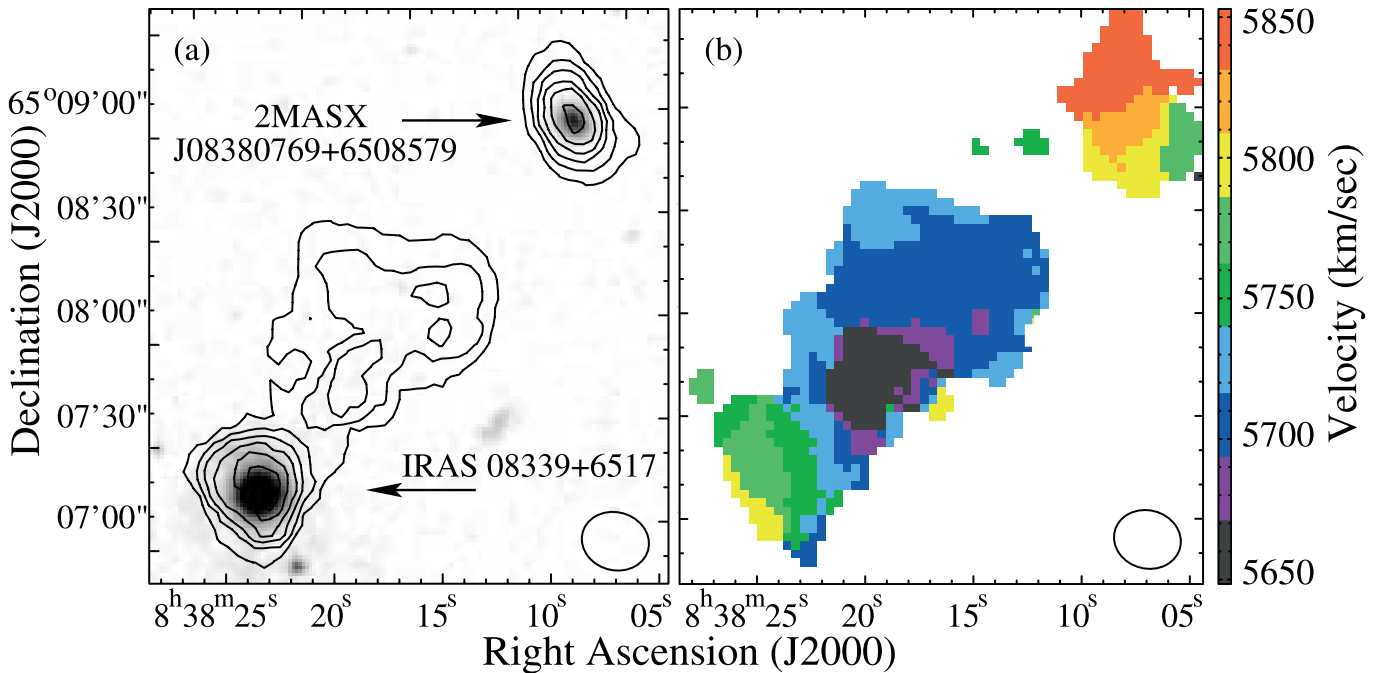


Fig. 2.—(a) DSS image of IRAS 08339+6517 overlaid with contours of the H I zeroth-moment image. Contours correspond to column densities of $(5.5, 15, 24, 33, 42, 51) \times 10^{20} \text{ cm}^{-2}$. Each galaxy is labeled; beam size is shown in the lower right corner. (b) Intensity-weighted velocity field of IRAS 08339+6517; it is apparent that H I is being removed from one or both systems. The companion galaxy appears to retain a component of solid-body rotation in neutral gas; clear signs of rotation are less prominent in IRAS 08339+6517 however, suggesting that this interaction has completely disrupted the neutral gas in this system. Beam size is shown in the lower right corner.

(DSS) optical image of Tol 1924–416, as well as an intensity-weighted velocity field. We detect a total integrated flux of $12.6 \pm 1.58 \text{ Jy km s}^{-1}$ from the Tol 1924–416 system. This compares well with the single-dish value of $11.4 \text{ Jy km s}^{-1}$ derived from Parkes telescope observations in the HIPASS Survey² (Barnes et al. 2001), suggesting that we have missed little or no flux because of the lack of zero-spacing interferometric elements. At the adopted distance of 37.5 Mpc, this corresponds to a total H I mass of $(4.2 \pm 0.5) \times 10^9 M_{\odot}$.

Inspecting the H I data cube allows us to measure the masses of neutral gas clearly associated with both Tol 1924–416 and with the companion ESO 338–IG04B. In the former we detect a total mass of $(1.4 \pm 0.2) \times 10^9 M_{\odot}$, and in the latter we find $(9.3 \pm 1.2) \times 10^8 M_{\odot}$. The remainder of the system mass, $(1.9 \pm 0.2) \times 10^9 M_{\odot}$ or $\sim 40\%$, is tidal material (see Fig. 1).

The velocity structures of Tol 1924–416 and ESO 338–IG04B have been studied in the H α line by Östlin et al. (1999, 2001). The agreement between the optical and radio velocity fields is very good. The radio data confirm the weak large-scale ordered rotation in Tol 1924–416 and the very ordered rotation in the companion system. Note that the H I associated with the Ly α -emitting system (Tol 1924–416) is spread out over $\sim 80 \text{ km s}^{-1}$ in radial velocity, suggesting that there is not a static screen of neutral gas along the line of sight to the starburst region.

Tol 1924–416 shows a variety of interesting characteristics in optical imaging. Östlin et al. (2003) used multicolor *HST*

images to derive the cluster formation history. The elevated star formation rate (\sim a few $M_{\odot} \text{ yr}^{-1}$) has been present for $\sim 40 \text{ Myr}$ and shows evidence for propagation throughout the disk. There appears to be little to no reddening in this system, in agreement with expectations based on the sample of LBGs in Shapley et al. (2003). While each of these parameters likely influence the propagation of Ly α photons through the ISM, our observations suggest that the ISM kinematics are also an important factor in this process.

The angular distance between the two galaxies is $\sim 6.6'$, corresponding to a minimum deprojected distance of $\sim 72 \text{ kpc}$. The total radial velocity extent is $\sim 150 \text{ km s}^{-1}$ ($V_{\text{sys}} = 2830 \text{ km s}^{-1}$), but components exist in both systems at the same velocities. Hence, it seems likely that these two systems may now be gravitationally bound. Regardless, the extended nature of the H I suggests that the present starburst in Tol 1924–416 likely was triggered by a strong gravitational interaction with ESO 338–IG04B and that the different star formation rates in these two otherwise similar systems (comparable H I masses [see above] and stellar masses [see Östlin et al. 2001]) are attributable to the recent tidal interaction between them.

3.2. IRAS 08339+6517

In Figure 2 we present contours of the zeroth-moment (total column density) image overlaid on a DSS optical image of IRAS 08339+6517, as well as an intensity-weighted velocity field. We detect a total integrated flux of $3.68 \pm 0.46 \text{ Jy km s}^{-1}$ from the IRAS 08339+6517 system; this compares well with the single-dish value derived from Nançay Observatory observations, $3.81 \text{ Jy km s}^{-1}$ (Martin et al. 1991), again suggesting negligible flux loss due to lack of zero-spacing baselines. At the adopted distance of 80 Mpc, this corresponds to a total H I mass of $(5.6 \pm 0.7) \times 10^9 M_{\odot}$.

² The Parkes telescope is part of the Australia Telescope, which is funded by the Commonwealth of Australia for operation as a National Facility managed by CSIRO. For HIPASS data see <http://www.atnf.csiro.au/research/multibeam/>.

We find $(1.1 \pm 0.2) \times 10^9 M_{\odot}$ of H I to be associated with IRAS 08339+6517. Its companion system, 2MASX J08380769+6508579, is found to have a total H I content of $(7.0 \pm 0.9) \times 10^8 M_{\odot}$, leaving the remaining $(3.8 \pm 0.5) \times 10^9 M_{\odot}$ to reside in tidal material between the two systems. This implies that the bulk of the neutral gas ($\sim 70\%$) in this interacting system has been removed from one or both galaxies. Interestingly, the peak single-plane column density is found in tidal material and is not associated with either galaxy.

Mas-Hesse et al. (2003) have shown, from the analysis of *HST* STIS high-resolution UV spectroscopy, that in front of the central ~ 5 kpc ($13''$) of this galaxy a column density of $\sim 10^{19.9} \text{ cm}^{-2}$ of neutral gas is outflowing with a velocity of around -300 km s^{-1} . This flow of material leaving the central area of IRAS 08339+6517 could be feeding the region between both galaxies. It is interesting to note that the neutral gas in this intermediate region is approaching us with an average velocity of around -100 km s^{-1} . However, no neutral gas is detected in the STIS observations at the systemic velocity of the galaxy ($V_{\text{sys}} = 5750 \text{ km s}^{-1}$), derived from these radio observations. This implies the existence of finer details in the velocity structure than can be inferred from these H I observations (e.g., an expanding shell powered by the starburst; see Mas-Hesse et al. 2003).

The distance of IRAS 08339+6517 (80 Mpc) precludes detailed optical studies of the stellar or cluster populations. Inferences about other intrinsic properties of the galaxy must therefore rely on spectral data. Gonzalez Delgado et al. (1998) measure an H α flux corresponding to a star formation rate of $\sim 8 M_{\odot} \text{ yr}^{-1}$ (applying the prescription of Kennicutt et al. 1994). The measured reddening reaches values as large as $E(B - V) = 0.5$ mag, suggesting substantial amounts of dust in this system. Again we note that these factors likely contribute to the propagation of Ly α photons. However, since this starburst region appears to suffer from substantial reddening, the importance of ISM kinematics in Doppler-shifting the Ly α photons out of resonance appears to be pronounced.

For a measured angular separation of $2.4''$, the implied minimum separation is 56 kpc. The H I radial velocity extent is $\sim 300 \text{ km s}^{-1}$, which suggests that the neutral gas surrounding IRAS 08339+6517 is highly turbulent, having been powered by the release of mechanical energy in the central starburst. At a smaller spatial scale the turbulence is still higher, as derived from UV spectroscopy (see Mas-Hesse et al. 2003).

While we can not definitively state that these galaxies now form a bound system, the effects of the gravitational interaction are pronounced in IRAS 08339+6517. Interestingly, this starburst system shows two peaks of Ly α emission in our ACS imaging and may be the remnant of an earlier merger in its own

right. On the other hand, the comparatively underluminous nature of 2MASX J08380769+6508579 (i.e., no obvious massive starburst episode in the current epoch) suggests that the effects of the interaction have not been as severe for the secondary system. Again, the less massive system appears to retain a strong component of solid-body rotation. IRAS 08339+6517 also appears to be undergoing organized rotation, but the neutral gas is spread out along the line of sight over $\sim 80 \text{ km s}^{-1}$.

4. CONCLUSIONS

VLA H I imaging of the starburst galaxies Tol 1924–416 and IRAS 08339+6517 is presented. These two systems are remarkably similar in H I content, mass, and current evolutionary state. In each, we find extended neutral gas between the target and nearby neighbors, suggesting that interactions have played an important role in triggering the massive starbursts in the primary galaxies. The close proximity of the companions suggests that the interactions were recent, and the similar velocities of both primary and secondary galaxies argues that these systems may end up gravitationally bound.

Since both primary systems are intense Ly α emitters, these data support the interpretation that the ISM kinematics are an important mechanism that affects the escape of Ly α photons from starburst regions. Combined with the results on LBGs (Shapley et al. 2003), these data have immediate implications for the use of the strength of Ly α emission in determining star formation rates, since the results will be dependent on the geometry of the ISM and other factors (e.g., dust, star formation rate) and not on properties inherent to the starburst being considered. Further H I observations of Ly α -emitting galaxies (and, conversely, of starburst systems with no apparent Ly α emission) are certainly warranted to further explore the role of the ISM in regulating the escape of Ly α photons from starburst environments.

Support for this work was provided by NASA through grant GO-9470 from the Space Telescope Science Institute, which is operated by AURA, Inc., under NASA contract NAS5-26555. J. M. C. is supported by NASA Graduate Student Researchers Program (GSRP) Fellowship NGT 5-50346. E. D. S. acknowledges partial support from NASA LTSARP grant NAG5-9221 and the University of Minnesota. This research has made use of the NASA/IPAC Extragalactic Database (NED), which is operated by the Jet Propulsion Laboratory, California Institute of Technology, under contract with the National Aeronautics and Space Administration, and NASA's Astrophysics Data System.

REFERENCES

- Barnes, D. G., et al. 2001, *MNRAS*, 322, 486
 Charlot, S., & Fall, S. M. 1993, *ApJ*, 415, 580
 Freedman, W. L., et al. 2001, *ApJ*, 553, 47
 Giavalisco, M., Koratkar, A., & Calzetti, D. 1996, *ApJ*, 466, 831
 Gonzalez Delgado, R. M., Leitherer, C., Heckman, T., Lowenthal, J. D., Ferguson, H. C., & Robert, C. 1998, *ApJ*, 495, 698
 Kennicutt, R. C., Tamblyn, P., & Congdon, C. E. 1994, *ApJ*, 435, 22
 Kunth, D., Leitherer, C., Mas-Hesse, J. M., Östlin, G., & Petrosian, A. 2003, *ApJ*, 597, 263
 Kunth, D., Lequeux, J., Sargent, W. L. W., & Viallefond, F. 1994, *A&A*, 282, 709
 Kunth, D., Mas-Hesse, J. M., Terlevich, E., Terlevich, R., Lequeux, J., & Fall, S. M. 1998, *A&A*, 334, 11
 Leitherer, C., Ferguson, H. C., Heckman, T. M., & Lowenthal, J. D. 1995, *ApJ*, 454, L19
 Leitherer, C., Li, I.-H., Calzetti, D., & Heckman, T. M. 2002, *ApJS*, 140, 303
 Lequeux, J., Kunth, D., Mas-Hesse, J. M., & Sargent, W. L. W. 1995, *A&A*, 301, 18
 Martin, J. M., Bottinelli, L., Gouguenheim, L., & Dennefeld, M. 1991, *A&A*, 245, 393
 Mas-Hesse, J. M., Kunth, D., Tenorio-Tagle, G., Leitherer, C., Terlevich, R. J., & Terlevich, E. 2003, *ApJ*, 598, 858
 Östlin, G., Amram, P., Bergvall, N., Masegosa, J., Boulesteix, J., & Márquez, I. 2001, *A&A*, 374, 800
 Östlin, G., Amram, P., Masegosa, J., Bergvall, N., & Boulesteix, J. 1999, *A&AS*, 137, 419
 Östlin, G., Bergvall, N., & Roenback, J. 1998, *A&A*, 335, 85
 Östlin, G., Zackrisson, E., Bergvall, N., & Rönnback, J. 2003, *A&A*, 408, 887
 Shapley, A. E., Steidel, C. C., Pettini, M., & Adelberger, K. L. 2003, *ApJ*, 588, 65
 Tenorio-Tagle, G., Silich, S. A., Kunth, D., Terlevich, E., & Terlevich, R. 1999, *MNRAS*, 309, 332